Power Flow Analysis and Critical Design Issues of Retrofit Light-Emitting Diode (LED) Light Bulb

Sinan Li, Huanting Chen, *Member, IEEE*, Siew-Chong Tan, *Senior Member, IEEE*, S. Y. (Ron) Hui, *Fellow, IEEE*, and Eberhard Waffenschmidt, *Senior Member, IEEE*

***Abstract*—For retrofit applications, some high-brightness light-emitting diode (LED) products have the same form factor restrictions as existing incandescent light bulbs. Such form factor constraints may restrict the design and optimal performance of the LED technology. In this paper, some critical design issues for commercial LED bulbs designed for replacing E27 incandescent lamps are quantitatively analyzed. The analysis involves power audits on such densely packed LED systems so that the amounts of power consumption in: 1) the LED wafer; 2) the phosphor coating; and 3) the lamp translucent cover are quantified. The outcomes of such audits enable R&D engineers to identify the critical areas that need further improvements in a compact LED bulb design. The strong dependence of the luminous output of the compact LED bulb on ambient temperature is also highlighted.**

***Index Terms*—Energy audit, light-emitting diode, photo-electro-thermal theory.**

I. Introduction

LIGHT-EMITTING diodes (LED) have emerged as an important lighting technology in a wide range of lighting applications such as displays, decorative lighting, and public lighting. The LED technology is attractive in terms of its long lifetime, mercury-free nature, high luminous efficacy, and ability to illuminate in wide range of colors [1], [2]. For general lighting applications, the high-brightness white LEDs (HB-LEDs) are expected to replace traditional light sources such as the incandescent and compact fluorescent lamps [3], [4], [5] in the retrofit market. While there are several ways to generate white light, the combined use of blue LED and yellow phosphor coating is the dominant approach in white LED technology because the blue LED has luminous efficacy much higher than red and green LEDs [1].

Among the light bulb products, E27 incandescent lamps are probably the most widespread lighting devices with the largest replacement market. E27 light bulbs have a standard form factor that has been used for several decades. Unlike the traditional incandescent lamps that use tungsten filaments with high melting temperature and without the need for any heatsink, LED is semiconductor device that has low melting temperature and therefore requires heatsink to keep the junction temperature below a certain temperature limit (typically 125 °C). Besides the thermal issue, LED has a thermal droop characteristic because its luminous efficacy decreases as the junction temperature increases [1]. Several attempts have been proposed to consider the interactions of the photometric, electric, and thermal aspects of LED devices [6]–[9]. Such thermal-dependent photometric behaviors have been characterized mathematically for LED systems by the photo-electro-thermal theory [7]. The variation of the luminous flux of a white phosphor-coated (PC) LED as a function of the forward current and junction temperature has also been described in [8]. In general, the luminous flux can be approximated as an asymmetric parabolic function of the LED power, obeying the following equation [7]:

$$\phi = \alpha_1 P_d - \alpha_2 P_d^2 - \alpha_3 P_d^3 \quad \text{for} \quad \phi > 0 \tag{1}$$

where φ is the luminous flux, α_1, α_2, and α_3 are positive coefficients; P_d is the LED power (that includes the effects of the LED forward current and its junction temperature).

Equation (1) can be used to elaborate some design challenges faced by high-power and compact LED designs such as E27 LED bulbs which has limited space for the heatsink. When the LED power is small (e.g., less than 1 W), the second and the third terms on the right-hand side of (1) are negligible. But as the LED power exceeds 1 W, these two negative terms become increasingly significant. The peak of this luminous flux equation will shift to the low-power end as the thermal resistance of the heatsink increases [6]. The lack of space for accommodating a large heatsink in an E27 light bulb is therefore a major constraint for LED product design.

Given such space limitation, there is not much understanding on the power distribution within compact LED light bulb design. In order to optimize E27 LED bulb or similar compact LED bulbs, it is necessary to understand the limitations of the product design posed by the standard structure of such product. An HB-LED system for general illumination usually comprises several functional stages:

1) LED ballast: it supplies electric power to the LED chips from the power source;
2) LED packages: they receive electric power from the ballast and radiate white light;

Manuscript received March 31, 2014; revised June 6, 2014; accepted July 4, 2014. Date of publication July 14, 2014; date of current version February 13, 2015. This work was supported by the Research Grant Council of Hong Kong under the Theme-Based Research Scheme (TBRS) T22-715/12N. Recommended for publication by Associate Editor J. M. Alonso.

S. Li, H. Chen, S.-C. Tan, and S. Y. (Ron) Hui are with the Department of Electrical and Electronic Engineering, The University of Hong Kong, Hong Kong (e-mail: sean861031@gmail.com; htchen23@gmail.com; sctan@eee.hku.hk; ronhui@eee.hku.hk).

E. Waffenschmidt is with the Faculty of Information, Media, and Electrical Engineering, Cologne University of Applied Sciences, Köln 50678, Germany.

Color versions of one or more of the figures in this paper are available online at http://ieeexplore.ieee.org.

Digital Object Identifier 10.1109/TPEL.2014.2339191

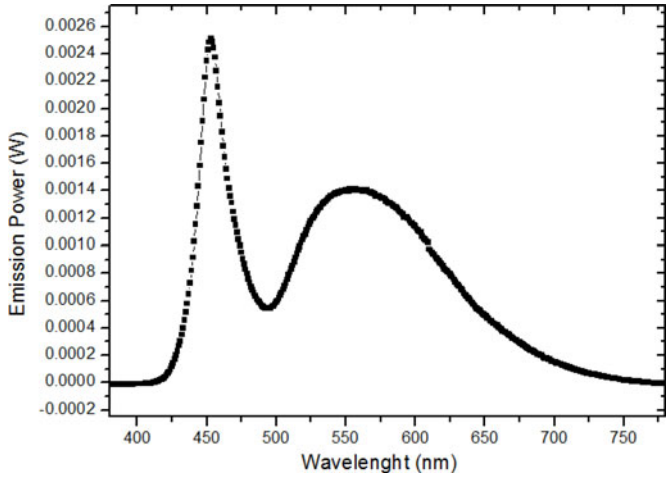

Fig. 1. Light spectrum of a phosphor-based white LED.

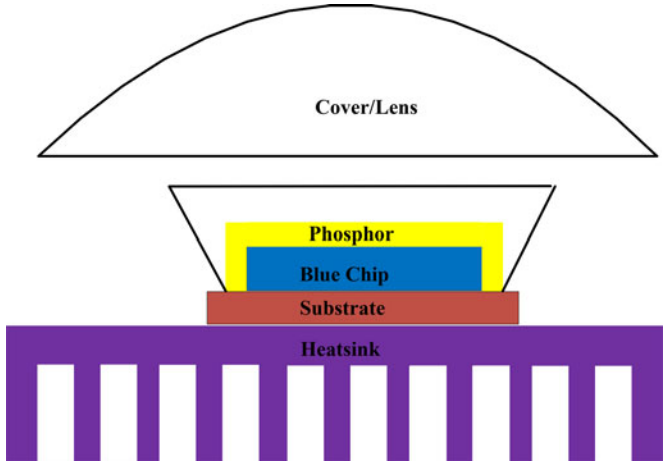

Fig. 2. Detailed inside view of the function stages of an LED package.

3) lamp cover or lens: it scatters the emitted light as a way to satisfy certain color temperature or viewing angle requirements. The optical power emitted from the LED chips is partially lost in this stage;
4) heatsink: it dissipates the heat generated from the ballast and the LEDs and all other heat sources.

Research in the chemical compositions [10]–[15] of the various types of phosphor coatings is beyond the scope of this paper. This paper focuses on the engineering design aspects of the LED devices used in compact LED bulbs from a system point of view. It involves an investigation into the power distributions of three PC white LED samples mounted inside a standard E27 LED bulb. It is an extended work of [16] which includes results of only one LED sample. Power audits on the LED wafer, phosphor coating, and translucent lens/cover have been conducted. While LED device researchers, electronic engineers, and production engineers usually focus on the device design, ballast design, and mechanical structure design respectively, the outcomes of such power audits based on a system approach provide insightful information for all stakeholders about effects of each component in the LED bulb structure and enable us to pinpoint critical design issues and scopes of improvements in future compact LED bulb designs.

II. Energy Flowchart and Power Audit of the LED System

This study focuses on power audits of an LED bulb based on the use of three types of PC white LED devices. Fig. 1 shows a typical light spectrum which consists of the sum of two spectra, namely one strong blue light spectrum generated directly from a GaN or InGaN LED at the 450 nm, and a second light spectrum of Stokes-shifted wavelengths emitted from the yellow phosphor coating. During the Stokes-shift process where the phosphor absorbs the blue photon energy and emits light of longer wavelengths, there is a loss of heat energy, commonly known as the Stokes-shift loss. A schematic of the interior structure is shown in Fig. 2. For simplicity, the phosphor-based LEDs can be perceived as having two power processing sub-stages: one being the blue LED chip generating blue light and the other being the phosphor layer performing the Stokes-shift process. Since the PC LED is still the most popular method of generating white light from LED [10], the following analysis will be based on the PC LED structures.

Based on Fig. 2, the energy flowchart can be drawn as shown in Fig. 3, which consists of five stages of energy conversion. Fig. 4 shows the photograph of the exterior and interior functional stages of the LED bulb.

In Stage 1, the input power P_{in} is processed by the LED ballast with an efficiency of $\eta_{\text{electrical}}$. An LED ballast could be of passive [17]–[19], linear or switched type [20]–[24]. Usually a single-staged switched-type ballast is employed in a compact LED system design due to their high-frequency operation and compact size. Usually, the ballast comprises an input diode bridge and a cascaded dc/dc converter. Depending on topologies and control methods, they can provide power factor correction (PFC) as well as galvanic isolation. Popular dc/dc topologies are buck, buck-boost, SEPIC (without isolation) as well as flyback and integrated single-stage topologies (with isolation). The power losses of those ballasts arise mainly from the switching loss, conduction loss, and core loss of magnetic components. For topologies without isolation, the duty ratio is very small and conduction loss on free-wheeling diode is high; for the ones with isolation, even though the duty ratio is moderate, but power is lost in the transformer's leakage inductance during each switching cycle. The power delivered to the LED chips from the ballast can be generalized as

$$P_d = P_{\text{in}}\eta_{\text{electrical}} \tag{2}$$

where P_d is the input power of the second stage.

In Stage 2, the blue LED chips convert electric energy into light energy by emitting blue light at an efficiency of η_1. The optical power of the blue LED, $P_{\text{opt(blue)}}$, is given as

$$P_{\text{opt(blue)}} = P_d\eta_1 \tag{3}$$

while the rest of the input power are converted into heat. The heat generation is related to several power-loss mechanisms, such as the leakage current power loss due to tunneling of electrons to

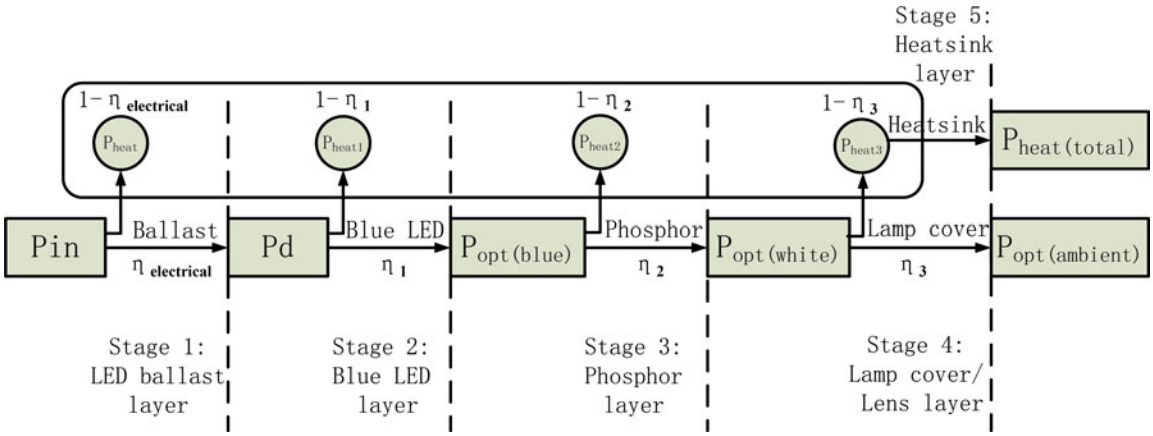

Fig. 3. Energy flowchart with the five functional stages of the LED system.

Fig. 4. Photographs of the exterior and interior functional stages of an LED bulb. (a) Ballast. (b) Heatsink. (c) Cover/lens. (d) LED bulb. (e) Shineon blue LED. (f) Shineon white LED. (g) Cree-XRE Blue LED. (h) Cree-XRE white LED. (i) Osram-W5AP Blue LED. (j) Osram-W5AP white LED.

the states of InGaN/GaN interfaces, power loss due to the effect of auger recombination, and power loss due to nonradiative recombination. Additionally, any photons generated by radiative recombination inside the LED chip may be emitted as external light or are trapped within the LED chip (caused by total internal reflection phenomenon of the semiconductor crystal), where they are finally absorbed and converted into heat. Taking all power losses into consideration, the total fraction of photons with respect to a known power level input that are emitted by the LED is known as the extraction efficiency η_1. Currently, the extraction efficiency of HB-LED is around 20%–40% [30], which is relatively much lower than other functional stages of energy conversion, and it is therefore the most influencing factor affecting the overall efficiency of the LED lamps.

In Stage 3, the blue light carrying a power of $P_{\mathrm{opt(blue)}}$ is converted into white light by the phosphor with a conversion power efficiency of η_2. The conversion power loss is related to the quantum efficiency and absorption characteristic of the phosphor materials, and is influenced by the trapping and absorption of the photons' energy, which is eventually converted into heat by the phosphor material of the PC LED. Currently, many commercially available phosphor materials are of good performance with a conversion efficiency η_2 of usually higher than 90%. The optical power of the emitted white light, $P_{\mathrm{opt(white)}}$, is given by

$$P_{\mathrm{opt(white)}} = P_{\mathrm{opt(blue)}}\eta_2. \tag{4}$$

Finally, the power of white light emitted from the PC LED will pass through Stage 4, which is the lamp cover or lens (blue

TABLE I
RELATIONSHIPS BETWEEN $k_{\rm opt}, k_h$ AND CONVERSION EFFICIENCIES η_1, η_2, η_3

Energy flow stage	$k_{\rm opt}$	k_h	η
2	$k_{\rm opt1} = \eta_1$	$k_{h1} = 1 - \eta_2$	$k_{\rm opt1}$
3	$k_{\rm opt2} = \eta_1\eta_2$	$k_{h2} = 1 - \eta_1\eta_2$	$k_{\rm opt2}/k_{\rm opt1}$
4	$k_{\rm opt3} = \eta_1\eta_2\eta_3$	$k_{h3} = 1 - \eta_1\eta_2\eta_3$	$k_{\rm opt3}/k_{\rm opt2}$

LED coated with phosphor epoxy is also a form of lenses), where the white light will be scattered to the ambient. For this stage, the lamp covers or lenses act as light filters, which in the process of scattering the light, partially trap photons within the covers/lenses converting them into extra heat, thereby incurring an additional form of optical power loss. Thus, the final optical output power of the light emitted to the ambient in terms of the lenses efficiency η_3, can be expressed as

$$P_{\rm opt(ambient)} = P_{\rm opt(white)}\eta_3. \tag{5}$$

In order to analyze the power flow of each functional stage, their energy conversion efficiencies η must be individually evaluated and compared. Practically, it is much easier to measure the optical power emitted from the respective stages than to measure the heat power dissipated form the stages. Hence, in the following discussion, the optical power coefficient $k_{\rm opt}$ is defined for each stage, which is the ratio of optical power $P_{\rm opt}$ over the total input power to LED P_d. In the same manner, the heat dissipation coefficient k_h is defined as the ratio of heat power $P_{\rm heat}$ (the power that finally ends up as heat in each stage) over P_d

$$k_{\rm opt} = P_{\rm opt}/P_d \tag{6}$$

$$k_h = P_{\rm heat}/P_d. \tag{7}$$

The coefficients $k_{\rm opt}$ and k_h can be used to derive the conversion efficiency η for each stage. For example, after Stage 2, the output optical power and heat power are

$$P_{\rm opt(blue)} = {\rm P}_d k_{\rm opt1} = P_d\eta_1 \tag{8}$$

$$P_{\rm heat1} = P_d k_{h1} = P_d - P_{\rm opt(blue)} = P_d(1-\eta_1). \tag{9}$$

Therefore

$$k_{\rm opt1} = \eta_1 \tag{10}$$

$$k_{h1} = 1 - \eta_1. \tag{11}$$

Using (10), the conversion efficiency η_1 can be calculated as

$$\eta_1 = k_{\rm opt1} = 1 - k_{h1}. \tag{12}$$

Following the same approach, the relationships between $k_{\rm opt}$, k_h and η for each stage can be derived and are tabulated in Table I.

It is evident from Table I that the higher the conversion efficiency η in each power conversion stage, the higher the $k_{\rm opt}$ and the lower the k_h. From Table I, the conversion efficiency η of each stage can be derived giving $k_{\rm opt1}$, $k_{\rm opt2}$, and $k_{\rm opt3}$. Detailed results are included and compared in Section III.

III. EXPERIMENTAL RESULTS OF AUDITING THE POWER OF AN LED BULB

Three types of commercially available PC white LED devices have been used for experimental evaluation in this study. For each type, two LED samples are used. One sample has the silicone cover and the phosphor coating removed and is labeled as the "blue LED." The other sample is the whole LED package and is labeled as the "white LED." The three types of LED devices are as follows:

1) shineon warm-white LED with a rated power of 8 W (multiple-chip package);
2) cree-XRE white LED with a rated power of 6 W (single-chip package);
3) osram-W5AP white LED with a rated power of 5 W (single-chip package).

The electrical, thermal, and optical parameters of the three LED samples are shown in Table II. It has an internal LED ballast and the bulb is comprised of all the five function stages as mentioned previously. Fig. 4 illustrates some pictures of the exterior and internal functional stages of the LED bulb used in this experiment. In order to compare the three different LED types, an external controllable current source is used to replace the original ballasts and drive the LED samples at different power levels up to their respective rated power. For the power audit, the experiments are conducted at the ambient temperature of 22 °C under free convection. Each of the six samples listed in Table II is mounted on the same heatsink [see Fig. 4(b)] which uses the same cover [see Fig. 4(c)] to form the LED bulb [see Fig. 4(d)]. For each setup, the external power supply drives the LED power to its rated value. For this reason, the energy efficiency of the ballast (i.e., Stage 1) is not considered in the power audits. Each steady-state measurement is obtained after the bulb has been operated for over 40 min.

Fig. 5 shows the measurement results of the power audit of the aforementioned LED bulbs for each stage and at different power level P_d. The power distribution is represented by the optical efficiency $k_{\rm opt}$ in each stage and is highlighted with different colors in the figure. A thinner layer of the area between any two adjacent stages signifies a lower conversion loss between these stages, i.e., higher efficiency during conversion. Take the Shineon LED [see Fig. 5(a)] as an example. In Stage 2, when $P_d = 7.22$ W (with LED conducting current of $I_{\rm LED} = 0.58A$), the output optical power of blue LED is 2.65 W (with $k_{\rm opt1} = 36.7\%$). After the phosphor conversion stage, i.e., Stage 3, some power is lost and the total optical power emitted in the form of white light drops to 1.99 W (with $k_{\rm opt2} = 27.6\%$). Moreover, after the lamp cover is mounted, the actual emitted optical power left is only 1.77 $W(k_{\rm opt3} = 24.5\%)$. If the optical power output is assumed to be proportional to the emitted luminous flux, one can then predict that the huge drop from $k_{\rm opt1}$ to $k_{\rm opt3}(12.1\%)$ results in a proportional amount of reduction in the output light intensity. Finally, by taking into consideration the power loss from the LED ballast, and assuming a typical ballast efficiency of $\eta_{\rm electrical} = 85\%$, the final energy efficiency in this LED system will be 20.8%. This result shows that around 21% of total input electric energy has been

TABLE II
LED SYSTEMS PARAMETERS

	I(A)	V(V)	E (lm/W)	k_h	k_e	$R_{\rm jc}\,(^\circ C/W)$
Blue Shineon LED—Fig. 4(e)	0.48	12.4	15.6	0.61	−0.0016	4.0
White Shineon LED—Fig. 4(f)	0.48	12.18	94.2	0.71	−0.0026	4.0
Blue Cree-XRE LED—Fig. 4(g)	0.35	6.522	28.3	0.70	−0.0013	8.0
White Cree-XRE LED—Fig. 4(h)	0.35	6.327	80.4	0.75	−0.0032	8.0
Blue Osram-W5AP LED—Fig. 4(i)	0.6	6.421	10.3	0.71	−0.0021	5.0
White Osram-W5AP LED—Fig. 4(j)	0.6	6.388	64.5	0.78	−0.0042	5.0

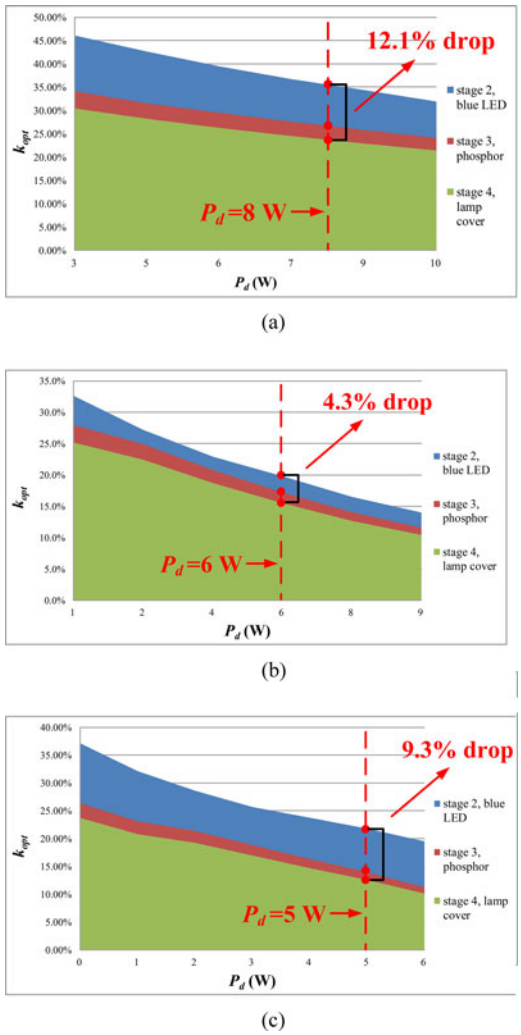

Fig. 5. Optical efficiency of the LED bulb for the respective stages. (a) Shineon LED. (b) Cree LED. (c) Osram-W5AP.

converted as light. The aforementioned analysis principle can also be applied to other two LED bulb samples.

Next, the efficiency performances of the respective functional stages for the three LED samples are compared. Following the stages in Table I, the energy efficiency of each stage as a function of LED power are plotted in Fig. 6. The following observations can be made:

1) For all three types of LED under consideration, the blue LED (in Stage 2) is the most inefficient power stage among the three stages. At the rated power of the devices of 8, 6, and 5 W, the efficiencies of the blue LED of Shineon, Cree, and Osram samples are about 36%, 18%, and 22%, respectively. These figures are below 40%.
2) The multiple-chip package (Shineon sample) has the best optical efficiency when compared with the single-chip packages (Cree and Osram samples). This feature has been explained previously in [25]. Multiple-chip package has a large contact area for the LED wafers for heat transfer, leading to lower thermal resistance of the LED package ($R_{\rm jc}$) and a smaller thermal droop characteristic (k_e) as indicated in Table II.
3) The optical efficiency of the phosphor layer can vary significantly (e.g., from about 58% to 90% in Fig. 6). Such efficiency seems to be temperature sensitive. For the multiple-chip sample with a wider surface area [see Fig. 6(a)], such efficiency is fairly constant with increasing power as the heat can be spread more evenly. But for the two single-chip samples [see Fig. 6(b) and (c)], the efficiency decreases, as the LED power and therefore temperature increases. Since this study does not consider the chemical compositions of the phosphor coatings, these results may point at two possibilities that need further research. First, the effects of temperature on the optical efficiency of the phosphor materials should be investigated. Second, if this temperature effect is a valid reason, the structure of the LED package (that affects the heat distribution) may play a part in reducing such thermal sensitivity.
4) In general, the optical efficiency of the lamp cover is independent of the temperature under the normal operating range.
5) The combined loss in the lamp cover and phosphor layer varies from 4.3% to 12.1% of their respective rated power levels (see Fig. 5) in the three samples. A good choice of lamp cover and phosphor layer will definitely make a noticeable difference in the overall efficiency of the LED bulb.

From the previous discussion and observations, it is evident that more efforts should be devoted to improving the conversion efficiency of the blue LED layer (Stage 2), and that there is more room for improvement for this stage than for the others. On one hand, research in new phosphor compositions with improved optical conversion efficiency is important. On the other hand, research in phosphor-free white LED design [26] should not be ignored because the scope of optical efficiency improvement is

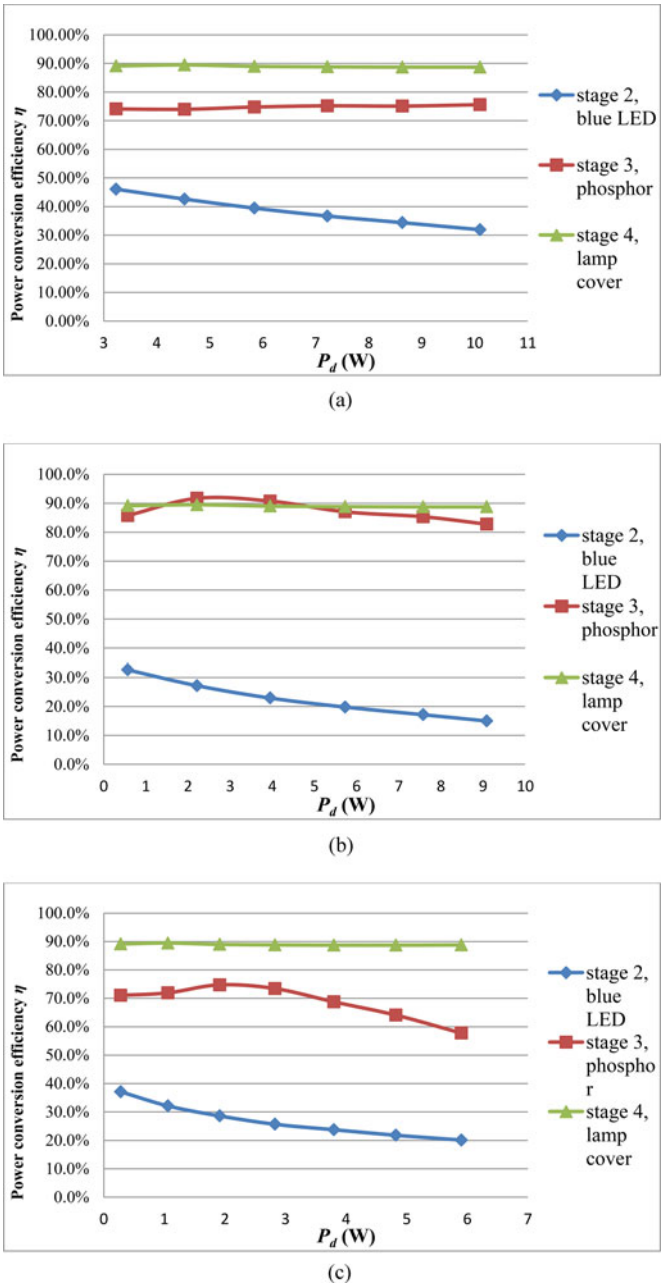

Fig. 6. Conversion efficiency of the LED bulb for Stage 2 to Stage 4.

still significant if the phosphor layer can be eliminated. As LED efficiencies are expected to improve continuously, the power audit information provided here can be used to predict the impact of improved LEDs on the total system efficiency.

IV. Impacts of Ambient Temperature on the Compact LED Bulb

Unlike incandescent lamps in which most of the heat energy from the filament is dissipated to the ambient in the form of infrared radiation (IR), heat energy within an LED bulb can only be dissipated through thermal conduction and convection, that is, from the active area (the LED p-n junction) to the underlying printed circuit board, then to the cooling system (such as heatsink), the housing, and finally to the ambient. Among LED, fluorescent and incandescent lamps, LED lamps have the most stringent requirements in thermal management because a large portion of heat has to be transferred through conduction and convection. If the thermal design is poor, heat energy will accumulate and heat up the p-n junction temperature of the LED, which will subsequently degrade the LED performance in terms of: 1) its lifetime; 2) its color property; 3) its luminous efficacy; and 4) the reliability of the overall LED system.

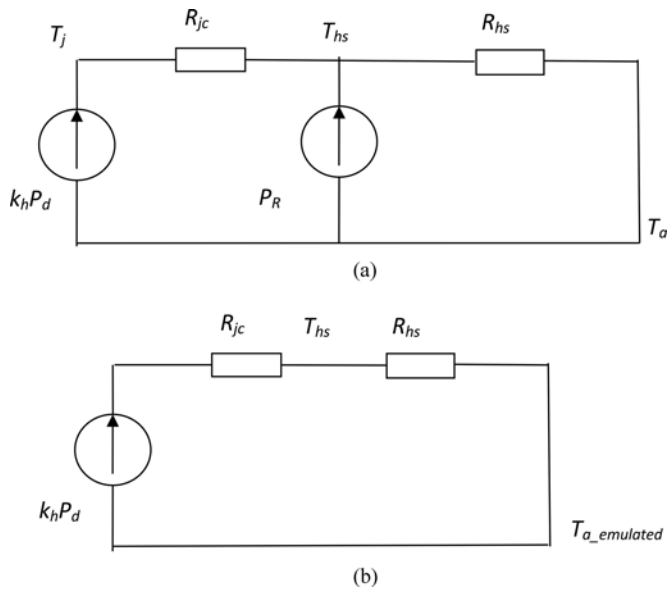

Fig. 7. (a) Equivalent thermal circuit including the heat sources of the LED chip and the extra heating resistor. (b) Equivalent thermal circuit of Fig. 8(a) with ambient temperature replaced by emulated ambient temperature.

Since LED bulbs can be placed in different lighting fixtures which may not have good ventilation, the effects of the ambient temperature on the luminous performance need to be examined. In order to test the LED bulb at different ambient temperature while its luminous output can still be measured inside the integrating sphere, a methodology has been devised to emulate the ambient temperature change. An extra heating resistor is mounted on the heatsink [see Fig. 4(d)] of the LED bulb so that resistive power dissipation can be controlled to vary the heatsink temperature. Fig. 7(a) shows the equivalent thermal circuit of the setup. The terms $k_h P_d$ and P_R represent the heat dissipation of the LED device and the heating resistor, respectively. The junction temperature of the LED can be represented as

$$T_j = k_h P_d R_{\rm jc} + (k_h P_d + P_R) R_{\rm hs} + T_a. \tag{13}$$

Rearranging (13) gives

$$T_j = k_h P_d (R_{\rm jc} + R_{\rm hs}) + P_R R_{\rm hs} + T_a. \tag{14}$$

By putting the emulated ambient temperature $T_{a\_\rm emulated}$ as

$$T_{a\_\rm emulated} = P_R R_{\rm hs} + T_a \tag{15}$$

equation (14) becomes

$$T_j = k_h P_d (R_{\rm jc} + R_{\rm hs}) + T_{a\_\rm emulated}. \quad (16)$$

The equivalent thermal circuit can now be represented as that shown in Fig. 7(b). Therefore, by manually controlling the power dissipation in the heating resistor, the equivalent ambient temperature can be altered and the LED bulb can be tested inside the integrating sphere at different emulated ambient temperature.

A. Temperature Effects on Luminous Flux

Based on this methodology, the LED bulb is tested at different equivalent ambient temperature. In the tests, the LED bulb is placed with the lens (i.e., translucent cover) of the bulb pointing downward. Measurements are made after the LED bulb has been operated for 40 min. The luminous flux is measured at different emulated ambient temperature over a range of electrical power. Fig. 8 displays four sets of luminous flux measurements at different ambient temperature for each of the three LED bulbs. Several important observations can be made.

The luminous flux decreases with increasing ambient temperature for the same rated power. For the sake of consumer benefits, LED bulb manufacturers should consider quoting the range of luminous flux for a certain range of ambient temperature. Such information will be valuable for lighting designers to design lighting systems to meet various illumination standards in different indoor and outdoor environments.

Even for a small heatsink for the E27 light bulb, LED device with multiple-chip structure and low thermal resistance can perform better than that with single-chip structure and high thermal resistance. Fig. 8(a) shows that the multiple-chip LED can work within the linear range up to the rated power of 8 W even when the ambient temperature is 93.3 °C. On the contrary, the two single-chip samples in Fig. 8(b) and (c) operate near the saturation region even when the ambient temperature is around 60 °C.

The parabolic shape of the flux-power curves recorded in–Fig. 8 has been explained by the PET theory [7], which predicts that the peak of the luminous flux curve occurs at the power P_d^*

$$P_d^* = -\frac{1 + k_e(T_a - T_o)}{2k_e k_h (R_{\rm jc} + NR_{\rm hs})} \quad \text{for} \quad P_d^* > 0 \text{ W} \quad (17)$$

where k_e is the coefficient of the rate of change of the luminous efficacy with junction temperature, T_o is typically set at 25 °C in LED data sheet and N is the number of LED mounted on the heatsink. In this case, $N = 1$ because only one LED device is tested in this experiment. Because the luminous efficacy decreases with increasing junction temperature, k_e is a negative coefficient. Therefore, the negative denominator of (17) and the minus sign indicate that the overall term in (17) is positive. For the retrofit LED bulb with compact heatsink, $R_{\rm hs}$ is fixed. According to (17), P_d^* decreases as T_a increases. This theoretical prediction agrees with the practical measurements shown in Fig. 8. For the small heatsink of Fig. 4(d), the thermal resistance $R_{\rm hs}$ is 6.5 °C/W. Such a large $R_{\rm hs}$ is typical and is a major design constraint for compact LED systems. In order to maximize the luminous flux, LED device with small $R_{\rm jc}$ and k_h should be chosen.

For the E27 retrofit LED bulb structure, it is interesting to note that P_d^* is located beyond the rated power of 8 W in Fig. 8. If dimming is required, the operating point will fall within the relatively linear part of the parabolic flux-power curves. The initial linear portion of the curves have good efficacy due to low junction temperature. This portion can be used for PWM dimming or *n*-level PWM dimming [27], since the light output by these two methods is similar to amplitude dimming due to the linear properties. Energy Star program suggests a continuous dimming range of 35%–100% for dimmable LED products [31]. The flux-power curves of Fig. 8 indicate that the E27 retrofit LED bulb can meet such requirement over a wide ambient temperature range.

B. Temperature Effects on Correlated Color Temperature and Color Rendering Index

Fig. 9 shows the measured correlated color temperature (CCT) of the LED bulbs. It is noted that the CCT increases with the increment of ambient temperature. The change of the ambient temperature will alter the junction temperature, which affects the CCT. According to the ANSI C78.377 [29], a nominal CCT of 3000 K should be within 3045 ± 175 K (i.e., within the range from 2870 to 3220 K), a nominal CCT of 5700 K should be within 5665 ± 355 K and a nominal CCT of 6500 K should be within 6530 ± 510 K. From Fig. 9, the measured CCT is within such range from low power to the rated power. The measured color rendering index (CRI) is recorded in Fig. 10. It is interesting to note that the CRI improves with increasing temperature. The measurements in Fig. 8 to Fig. 10 show that the luminous flux of the LED bulb is much more sensitive to ambient temperature change than the CCT and CRI.

C. Temperature Effects Due to the Position of the LED Bulb

Tests are also conducted with the LED lens pointing upward. In such position, heat generated by various functional stages will be trapped inside the bulb cover, resulting in an increase in junction temperature of the LED chip. The luminous flux, CCT and CRI measurements have been recorded and compared with the corresponding results obtained with the LED lens pointing downward. Fig. 11 shows that the luminous flux will be reduced in the upward position. This is expected because the rise in the junction temperature will reduce luminous efficacy and therefore the luminous flux. However, the junction temperature rise does not significantly affect the CCT and CRI. It is noted in Fig. 12 that the CCT of Shineon LED will slightly increase, but such increase is within 10 K, which is too small to be noticed by human eyes. For the Cree-XRE and Osram-W5AP LED samples, the CCT and CRI will obviously increase, which shall be noticed by human eyes. Fig. 13 indicates that the difference in CRI for the upward and downward positions is also small. Therefore, the orientation of the compact LED bulb affects its

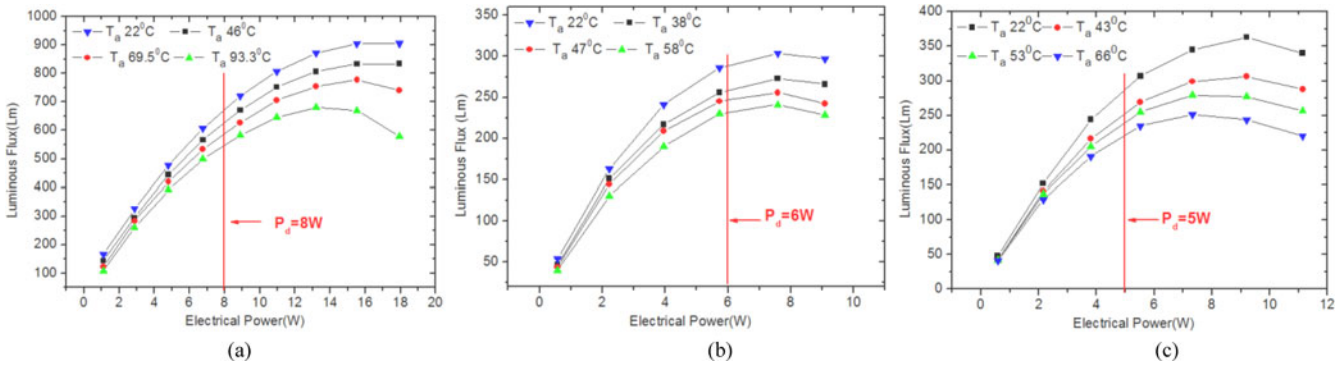

Fig. 8. Measured luminous flux with the LED bulb in the downward position. (a) Shineon LED. (b) Cree-XRE LED. (c) Osram-W5AP.

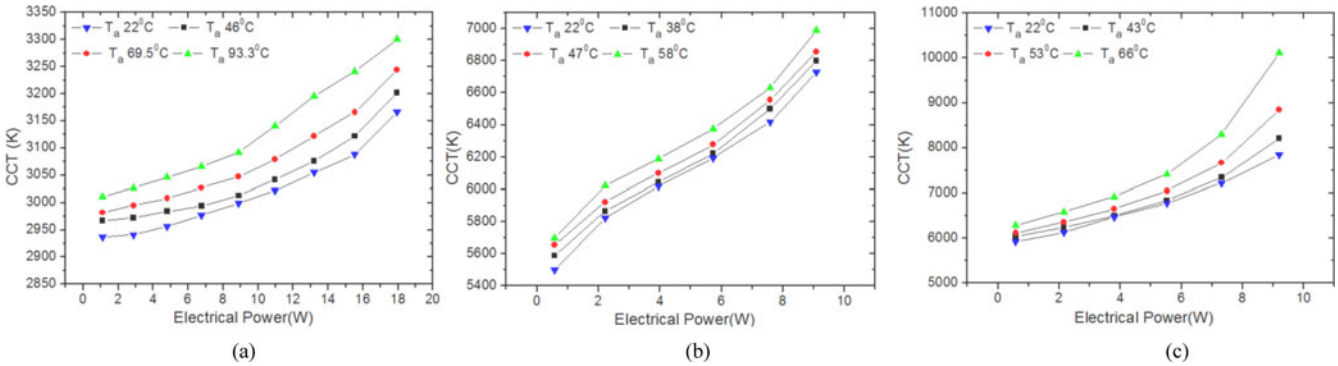

Fig. 9. Measured correlated color temperature (CCT) with the LED bulb in the downward position. (a) Shineon LED. (b) Cree-XRE LED. (c) Osram-W5AP.

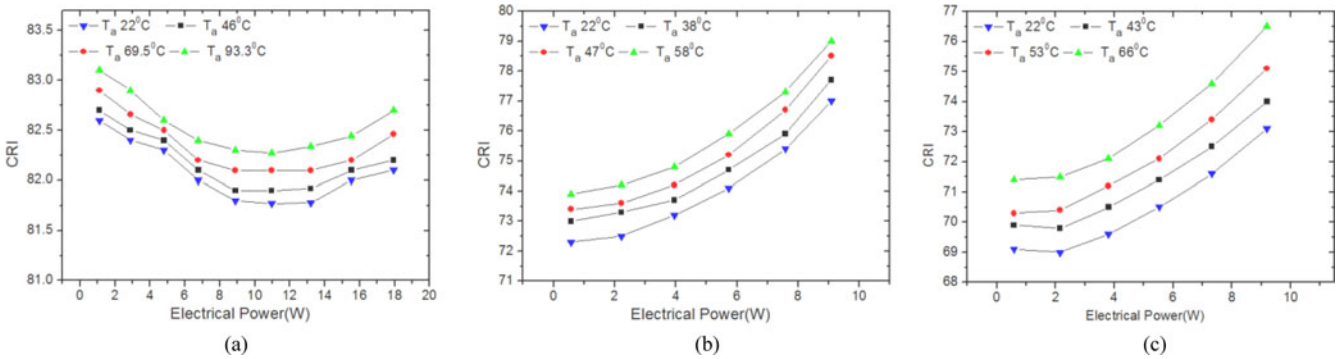

Fig. 10. Measured color rendering index (CRI) with the LED bulb in the downward position. (a) Shineon LED. (b) Cree-XRE LED. (c) Osram-W5AP.

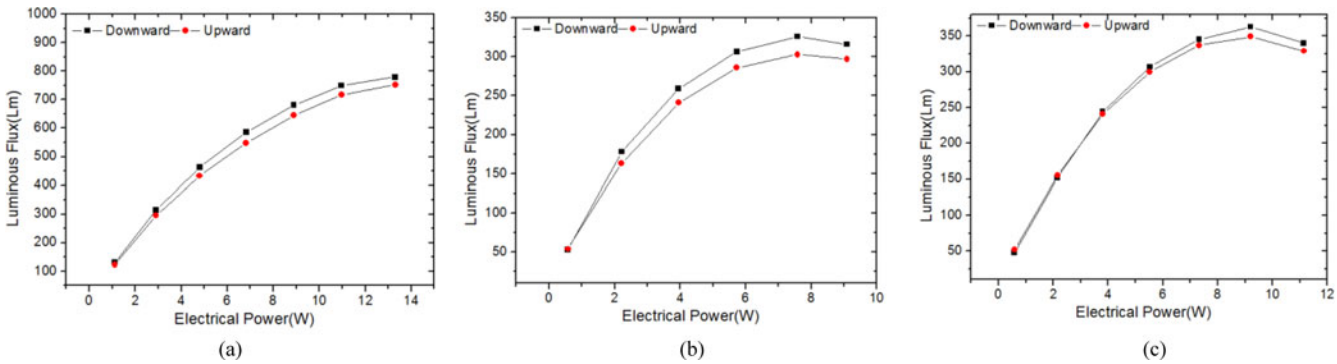

Fig. 11. Measured luminous flux. (a) Shineon LED. (b) Cree-XRE LED. (c) Osram-W5AP.

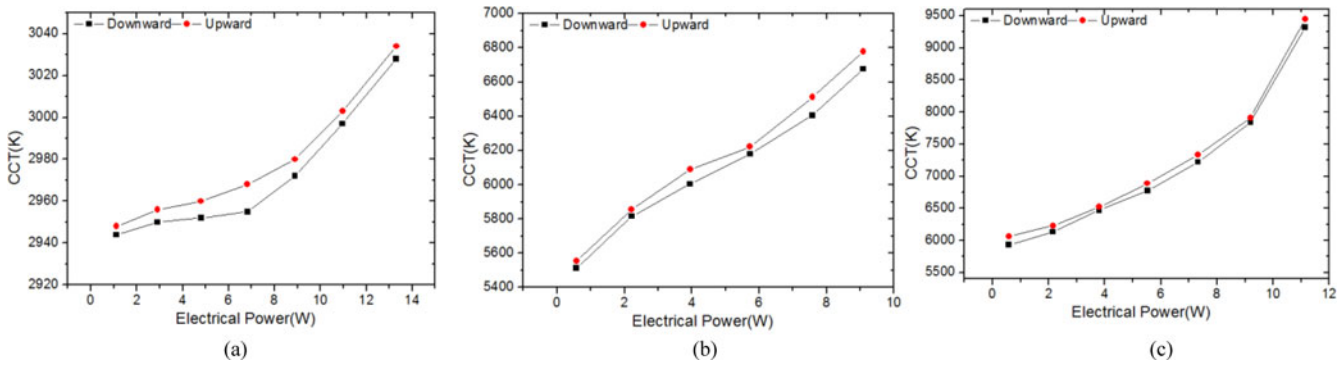

Fig. 12. Measured correlated color temperature (CCT). (a) Shineon LED. (b) Cree-XRE LED. (c) Osram-W5AP.

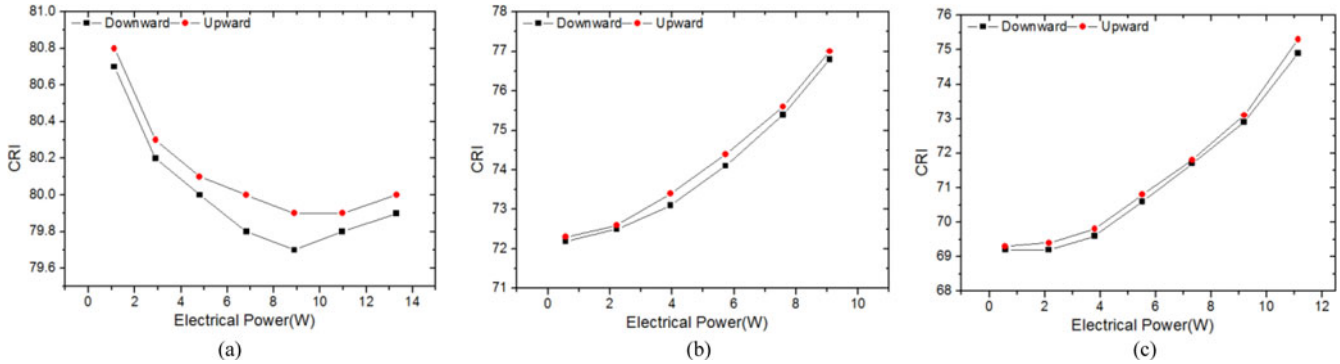

Fig. 13. Measured color rendering index (CRI). (a) Shineon LED. (b) Cree-XRE LED. (c) Osram-W5AP.

luminous flux more than its CCT and CRI from a user's point of view.

V. Conclusion

Critical design issues of a compact LED light bulb are addressed. A power flow analysis has been conducted on E27 retrofit LED bulbs based on three different LED devices to quantify the energy efficiencies of several functional stages, including the blue LED, the phosphor layer and the lens/lamp cover layer. The power audits show that the blue LED stage has the lowest energy efficiency, even though blue LED is more efficient than red and green LEDs. The power audit analysis provides information for researchers and design engineers to investigate the scope of efficiency improvement can be targeted in each functional stage. The thermal effects due to the constraint of the small heatsink in compact LED system affect the luminous flux more than the CCT and CRI. Experimental results indicate that the luminous flux is much more sensitive to ambient temperature change, while the CCT and CRI variations with temperature are relatively small. In order to improve the luminous performance, LED devices with small k_h and $R_{\rm jc}$, and phosphor coating and lens with high conversion efficiency should be chosen. Although the power audits do not include the driver circuit, it is envisaged that LED driver without using electrolytic capacitor should be designed in order to prolong the lifetime of the driver in a compact design with stringent constraint on the cooling mechanism.

References

[1] E. Schubert, T. Gessmann, and J. Kim, *Light Emitting Diodes*, 2nd ed. Cambridge, U.K.: Cambridge Univ. Press, 2006.

[2] M. Harris, "Let there be light," *IET Eng. Technol. Mag.*, vol. 4, no. 20, pp. 18–21, Nov./Dec. 2009.

[3] (2013, Feb.). Varying approaches to LED retrofit lamps show no limit. *LEDs Magazine*. [Online]. Available: http://www.ledsmagazine.com/articles/print/volume-10/issue-2/features/varying-approaches-to-led-retrofit-lamps-show-no-limit-magazine.html

[4] J. M. Alonso, D. Gacio, A. J. Calleja, J. Ribas, and E. L. Corominas, "A study on LED retrofit solutions for low-voltage halogen cycle lamps," *IEEE Trans. Ind. Appl.*, vol. 48, no. 5, pp. 1673–1682, Sep./Oct. 2012.

[5] Y. K. Cheng and K. W. E. Cheng, "General study for using LED to replace traditional lighting devices," in *Proc. 2nd Int. Conf. Power Electron. Syst. Appl.*, 2006. pp. 173–177.

[6] P. Baureis, "Compact modeling of electrical, thermal and optical LED behavior," in *Proc. 35th Eur. Solid-State Device Res. Conf.*, Grenoble, France, Sep. 2005, pp. 145–148.

[7] S. Y. (Ron) Hui and Y. X. Qin, "A general photo-electro-thermal theory for light emitting diode (LED) systems," *IEEE Trans. Power Electron.*, vol. 24, no. 8, pp. 1967–1976, Aug. 2009.

[8] X. H. Tao and S. Y. R. Hui, "Dynamic photo-electro-thermal theory for light-emitting diode systems," *IEEE Trans. Ind. Electron.*, vol. 59, no. 4, pp. 1751–1759, Apr. 2012.

[9] H. T. Chen, X. H. Tao, and S. Y. R. Hui, "Estimation of optical power and heat dissipation coefficient for the photo-electro-thermal theory for LED systems," *IEEE Trans. Power Electron.*, vol. 27, no. 4, pp. 2176–2183, Apr. 2012.

[10] A. A. Setlur, "Phosphors for LED-based solid-state lighting," *Electrochem. Soc. Interface*, pp. 32–36, Winter 2009.
[11] K. H. Lee and S. W. R. Lee, "Process development for yellow phosphor coating on blue light emitting diodes (LEDs) for white light illumination," in Proc. 8th Electron. Packag. Technol. Conf., 2006, pp. 379–384.
[12] D. Bera, S. Maslov, L. Qian, J. S. Yoo, and P. H. Holloway, "Optimization of the yellow phosphor concentration and layer thickness for down-conversion of blue to white light," *J. Display Technol.*, vol. 6, no. 12, pp. 645–651, 2010.
[13] Z. Liu, S. Liu, K. Wang, and X. Luo, "Optical analysis of phosphor's location for high-power light-emitting diodes," *IEEE Trans. Device Mater. Rel.*, vol. 9, no. 1, pp. 65–73, Mar. 2009.
[14] R. Hu, H. Zheng, J. Hu, and X. Luo, "Comprehensive study on the transmitted and reflected light through the phosphor layer in light-emitting diode packages," *J. Display Technol.*, vol. 9, no. 6, pp. 447–452, 2013.
[15] R. Hu and X. Luo, "A model for calculating the bidirectional scattering properties of phosphor layer in white light-emitting diodes," *J. Lightw. Technol.*, vol. 30, no. 21, pp. 3376–3380, 2012.
[16] S. Li, H. Chen, S. C. Tan, S. Y. R. Hui, and E. Waffenschmidt, "Critical design issues of retrofit light-emitting diode (LED) light bulb," in *Proc. 29th Annu. IEEE Appl. Power Electron. Conf. Expo.*, 2014, pp. 531–536.
[17] J. M. Alonso, S. S. Member, D. Gacio, A. J. Calleja, J. Ribas, and E. L. Corominas, "A study on LED retrofit solutions for low-voltage halogen cycle lamps," *IEEE Trans. Ind. Appl.*, vol. 48, no. 5, pp. 1673–1682, Sep. 2012.
[18] H. Kim, B. Lee, and C.-T. Rim, "Passive LED driver compatible with rapid-start ballast," in *Proc. 8th Int. Conf. Power Electron.—ECCE Asia*, 2011, pp. 507–514.
[19] S. Y. Hui, S. N. Li, X. H. Tao, W. Chen, and W. M. Ng, "A novel passive offline LED driver with long lifetime," *IEEE Trans. Power Electron.*, vol. 25, no. 10, pp. 2665–2672, Oct. 2010.
[20] Y. Qin, H. Chung, D. Y. Lin, and S. Y. R. Hui, "Current source ballast for high power lighting emitting diodes without electrolytic capacitor," in *Proc. IEEE 34th Annu. Conf. Ind. Electron.*, 2008, pp. 1968–1973.
[21] X. Qu, S. C. Wong, and C. K. Tse, "Resonance-assisted buck converter for offline driving of power led replacement lamps," *IEEE Trans. Power Electron.*, vol. 26, no. 2, pp. 532–540, Feb. 2011.
[22] J. M. Alonso, J. Vina, D. G. Vaquero, G. Martinez, and R. Osorio, "Analysis and design of the integrated double buck–boost converter as a high-power-factor driver for power-LED lamps," *IEEE Trans. Ind. Electron.*, vol. 59, no. 4, pp. 1689–1697, Apr. 2012.
[23] B. Wang, X. Ruan, K. Yao, and M. Xu, "A method of reducing the peak-to-average ratio of LED current for electrolytic capacitor-less AC–DC drivers," *IEEE Trans. Power Electron.*, vol. 25, no. 3, pp. 592–601, Mar. 2010.
[24] C. K. Tse, M. H. L. Chow, and M. K. H. Cheung, "A family of PFC voltage regulator configurations with reduced redundant power processing," *IEEE Trans. Power Electron.*, vol. 16, no. 6, pp. 794–802, Nov. 2001.
[25] Y. X. Qin and S. Y. R. Hui, "Comparative study on the structural designs of LED devices and systems based on the general photo-electro-thermal theory," *IEEE Trans. Power Electron.*, vol. 25, no. 2, pp. 507–513, Feb. 2010.
[26] Y. F. Cheung and H. W. Choi, "Color-tunable and phosphor-free white-light multilayered light-emitting diodes," *IEEE Trans. Electron. Devices*, vol. 60, no. 1, pp. 333–338, Jan. 2013.
[27] S.-C. Tan, "General n-level driving approach for improving electrical-to-optical energy-conversion efficiency of fast-response saturable lighting devices," *IEEE Trans. Ind. Electron.*, vol. 57, no. 4, pp. 1342–1353, Apr. 2010.
[28] *ENERGY STAR Program Requirements for Solid State Lighting Luminaires, Eligibility Criteria—Version 1.1*, 2008. [Online]. Available: http://www.energystar.gov/index.cfm?c=new_specs.ssl_luminaires
[29] American National Standard, Specifications for Chromaticity of Solid State Lighting Products, ANSI C78.377, 2008.
[30] Extracting more light from LEDs, Rensselaer Polytechnic Institute, Lighting Research Center. [Online]. Available: http://www.lrc.rpi.edu/programs/solidstate/cr_lightExtraction.asp
[31] Energy STAR Program Requirements Product Specification for Luminaries (Light Fixtures), Eligibility Criteria - version 1.1, 2012. [Online]. Available: http://www.energystar.gov/ia/partners/product_specs/program_reqs/Final_Luminaires_Program_Requirements.pdf

Sinan Li was born in China, in 1986. He received the B.S. degree in electrical engineering from Harbin Institute of Technology, Harbin, China, in 2009. He received the Ph.D. degree from the Department of Electrical and Electronic Engineering, The University of Hong Kong, Hong Kong.

He is the coinventor of an automatic reconfigurable current mirror technique. His current research areas include the design and analysis of power supplies, LED characteristics, and its relevant system designs.

Huanting Chen (M'13) received the Ph.D. degree in radio physics from Xiamen University, Xiamen, China, in 2010, and was a joint Ph.D. student at the Light and Lighting Laboratory, Catholic University College Gent, Belgium, from November 2009 to May 2010.

He was a Senior Research Associate in the Department of Electronic Engineering, City University of Hong Kong, Hong Kong, in 2011. He is currently a Postdoctoral Fellow in the Department of Electrical and Electronic Engineering, The University of Hong Kong. His research interest includes solid-state lighting theory and technology.

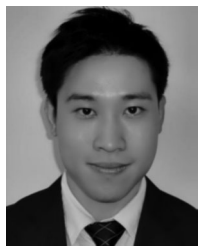

Siew-Chong Tan (S'00–M'06–SM'11) received the B.Eng. (Hons.) and M.Eng. degrees in electrical and computer engineering from the National University of Singapore, Singapore, in 2000 and 2002, respectively, and the Ph.D. degree in electronic and information engineering from the Hong Kong Polytechnic University, Hong Kong, in 2005.

From October 2005 to May 2012, he was a Research Associate, Postdoctoral Fellow, Lecturer, and an Assistant Professor in the Department of Electronic and Information Engineering, Hong Kong Polytechnic University, Hong Kong. From January to October 2011, he was a Senior Scientist at the Agency for Science, Technology and Research (A∗Star), Singapore. He is currently an Associate Professor in the Department of Electrical and Electronic Engineering, The University of Hong Kong, Hong Kong. He was a Visiting Scholar at Grainger Center for Electric Machinery and Electromechanics, University of Illinois at Urbana-Champaign, Champaign, USA, from September to October 2009, and an Invited Academic Visitor of Huazhong University of Science and Technology, Wuhan, China, in December 2011.

Dr. Tan serves extensively as a reviewer for various IEEE/IET transactions and journals on power, electronics, circuits, and control engineering. He is a coauthor of the book *Sliding Mode Control of Switching Power Converters: Techniques and Implementation* (Boca Raton, FL, USA: CRC, 2011). His research interests include power electronics and control, LED lightings, smart grids, and clean energy technologies.

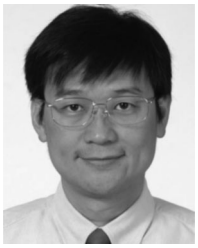

S. Y. (Ron) Hui (M'87–SM'94–F'03) received the B.Sc. (Eng.) (Hons.) from the University of Birmingham, in 1984 and the D.I.C. and Ph.D. degrees from Imperial College London, London, U.K., in 1987.

He has previously held academic positions at the University of Nottingham (1987–1990), University of Technology Sydney (1991–1992), University of Sydney (1992–1996), and the City University of Hong Kong (1996–2011). He currently holds the Chair Professorships at the University of Hong Kong and Imperial College London. He has published more than 200 technical papers, including more than 170 refereed journal publications and book chapters. More than 55 of his patents have been adopted by the industry.

Dr. Hui has been an Associate Editor of the IEEE TRANSACTIONS ON POWER ELECTRONICS since 1997 and an Associate Editor of the IEEE TRANSACTIONS ON INDUSTRIAL ELECTRONICS since 2007. He has been appointed twice as an IEEE Distinguished Lecturer by the IEEE POWER ELECTRONICS SOCIETY in 2004 and 2006, respectively. He served as an AdCom Member of the IEEE POWER ELECTRONICS SOCIETY and was the Chairman of its constitution and by-laws committee from 2002 to 2010. He received the Excellent Teaching Award in 1998 and the Earth Champion Award in 2008. He received an IEEE Best Paper Award from the IEEEIAS Committee on production and applications of light in 2002, and two IEEE Power Electronics Transactions Prize Paper Awards for his publications on wireless charging platform technology in 2009, and on LED system theory in 2010. His inventions on wireless charging platform technology underpin key dimensions of Qi, the world's first wireless power standard, with freedom of positioning and localized charging features for wireless charging of consumer electronics. In November 2010, he received the IEEE Rudolf Chope R&D Award from the IEEE Industrial Electronics Society, the IET Achievement Medal (The Crompton Medal) and was elected to the Fellowship of the Australian Academy of Technological Sciences and Engineering. He is the recipient of the 2015 IEEE William E. Newell Power Electronics Award.

Eberhard Waffenschmidt (A'05–M'07–SM'10) received the Ph.D. degree in electronic engineering from the Technical University (RWTH), Aachen, Germany.

From 1995 to 2011, he was with the Philips Research, as a Senior Scientist. Since September 2011 he has been a Professor of electrical power grids at the Cologne University of Applied Science. He is currently with the Philips Research as a consultant. At Philips, he worked on power electronics, especially on the integration of passive components and on wireless power transmission. He is involved in the research on power drivers for energy efficient LED lamps, especially in dc grids. His research interests include the demand on a power grid with high content of decentralized renewable generation of energy.